

Analysis and experimental verification of dual star permanent magnet synchronous motor with rotor back iron made of soft magnetic composite

Abstract. The research conducted at Poznan University of Technology with cooperation the Tele- and Radio Research Institute deals with finite element analysis of six-phase, dual star permanent magnet synchronous motor. To reduce eddy current losses in the rotor of the machine the rotor back iron segments have been made of soft magnetic composite (SMC). SMC are composites of iron powder particles separated with an electrically insulated layer. This technology has many advantages in relation to classical laminated core solutions; among other lower manufacturing costs due to simpler technology and reduced eddy current losses out of order times lower conductivity. The mathematical model of machine utilizes field circuit approach assuming planar symmetry of the machine. The magnetic properties of the applied SMC material have been introduced into the model basing on BH curves and unit losses vs. frequency characteristics measured at Tele- and Radio Research Institute. Accuracy of developed numerical model has been verified by measurements of the machine performance under normal and drive fault conditions tested on the elaborated research stand.

Streszczenie. prezentowane badania, prowadzone na Politechnice Poznańskiej we współpracy z Instytutem Tele- i Radiotechnicznym dotyczą analizy i weryfikacji eksperymentalnej sześciofazowego silnika synchronicznego z magnesami stałymi. W celu ograniczenia strat związanych z występowaniem prądów wirowych w obwodzie magnetycznym wirnika maszyny jego segmnty wykonano z miękkiego kompozytu magnetycznego (SMC). W stosunku do powszechnie stosowanych rdzeni laminowanych technologia proszkowych materiałów SMC posiada wiele zalet. Między innymi dzięki znacznie większej rezystywności materiały te pozwalały ograniczyć straty wiroprowadne w rdzeniu, a dzięki uproszczeniu technologii wytwarzania możliwe jest ograniczenie kosztów produkcji. W połowie obwodowym modelu maszyny założono symetrię płaszczyznową obwodu magnetycznego maszyny oraz uwzględniono magnetyczne właściwości zastosowanego materiału SMC na podstawie krzywych BH oraz charakterystyk stratności zmierzonych w Instytucie Tele- i Radiotechnicznym. Dokładność opracowanego modelu numerycznego została zweryfikowana poprzez pomiary wybranych parametrów testowanej maszyny przeprowadzone na opracowanym stanowisku badawczym. **Analiza i weryfikacja eksperymentalna sześciofazowego silnika synchronicznego z magnesami stałymi**

Keywords: multiphase permanent magnet synchronous motor, multi-inverter supply, finite element analysis.

Słowa kluczowe: wielofazowa maszyna z magnesami trwałymi, falownik wielofazowy, metoda elementów skończonych.

Introduction

In the recent years increased interest in permanent magnet synchronous machines (PMSM) with fractional slot contracted windings (FSCW) can be observed in many research teams [1,2]. By shorten end windings (in relation to machines of distributed windings) such machines offers possibility to reduce the copper losses and thus increase of efficiency with simultaneous winding cost reduction. The advantages of FSCW PMSM are especially apparent in case of low speed and high torque machines as direct drives or windmill generators [1]. Nevertheless the PMSM with FSCW suffer of parasitic effects as increased eddy current losses and torque ripples [3] and high level of magnetic noise [6]. These parasitic effects are mainly caused by high level of sub and super harmonics content in spatial distribution of the magnetomotive force (MMF) excited by such type of winding [3,6]. One of the methods to reduce level of distortion of the MMF spatial distribution is to increase the number of phases of the winding [2]. On the other hand the eddy current losses in the rotor can be reduced by using appropriate material for the construction of rotor magnetic circuit. In the presented contribution a dual three-phase machine with rotor yoke made of SMC material has been proposed. The machine performance has been studied by means of finite element method (FEM). The usefulness and accuracy of the elaborated model has been verified by comparing the simulation results with the measurements of selected parameters of the designed and build test machine. The measurements have been performed on the special designed research test stand. Developed research stand consists of the studied machine driven by specialized six phase inverter controlled by the ALS-1369 DSP based control system, data acquisition system (DAQ) based on the National Instrument NI9220 DAQ card and the DC power system utilizing dual channel

TTIQPX600DP programmable DC supply. The view of the rotor of studied machine has been shown in Fig. 1.

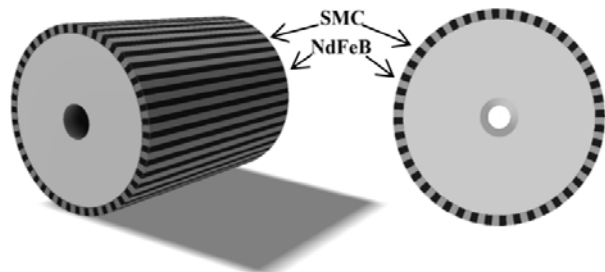


Fig.1. Spoke type magnet SMC based rotor of the machine

The rotor of the machine is composed of wedges made of the Somaloy 500 - the SMC concept brand of Swedish company Höganäs - and NdFeB sintered magnets magnetized as shown in Fig. 2.

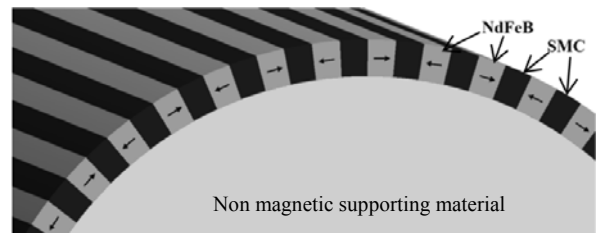


Fig.2. Rotor structure and direction of magnetization of permanent magnets

The applied rotor structure, i.e. spoke type topology of the permanent magnets arrangement allows to reduce the rotor inertia (by using lightweight supporting structure) with simultaneous high value of the magnetic flux density in the air gap of the machine.

Soft magnetic composite - Somaloy 500

The main component of the magnetic composites is the magnetic powder that could be obtained by mechanical or physicochemical methods, such as, e.g., milling of magnetic alloys or by atomization of materials from liquid phase [4]. Soft magnetic powders are generally produced by atomization of liquid metal or its alloy. Magnetic powder grains could be coated with a binder during the powder preparing process or alternatively — a mixture of magnetic powder, a binder, and a lubricant are prepared. Binders are used in the preparing of magnetic composites in order to bond powder grains. Binders are dielectrics and create an insulating layer on a surface of powder grains [5]. For the construction of the SMC wages used powder Somaloy 500 + 0,6% LB1 (see scanning electron microscope (SEM) images shown in Fig. 3).

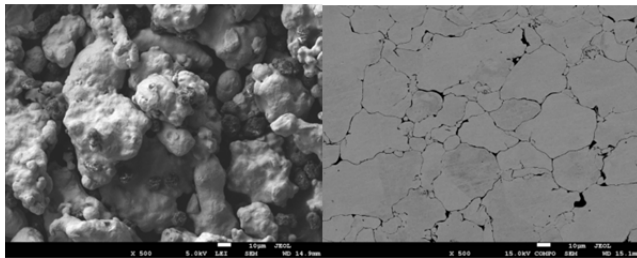


Fig.3. SEM of Somaloy 500 + LB1 powder – before and after the forming process

Powder types of Somaloy 500 are based on iron powder with an ultra-fine insulating layer - see SEM images shown in Fig. 3. Iron powder is mixed with 0.6% binder and lubricant (LB1). The insulating layer allows to obtain a relatively high material resistance, which is an undoubtedly advantage. Therefore, SMC materials can be used at frequencies up to 100 kHz, and a cross-over point for core losses for it and silicon steel (3% silicon content) is between 200 Hz to 400 Hz - see specific losses vs. flux density and frequency characteristics shown in Fig. 5 [8]. Whereas the magnetic permeability of the composite is lower and therefore the apparatus design of the SMC needs to take account of the magnetization curve (see Fig. 4).

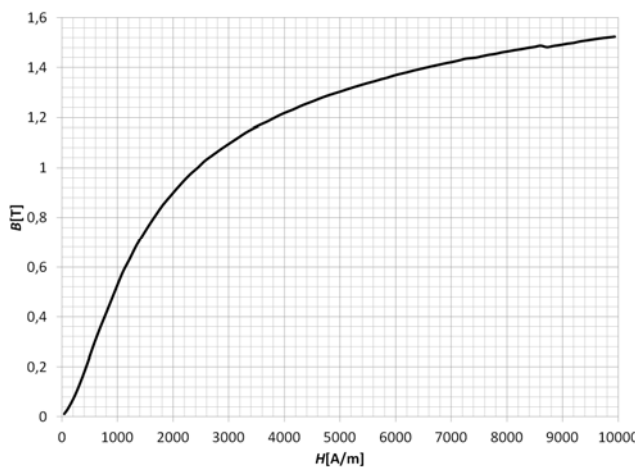


Fig.4. Magnetization characteristic of the Somaloy 500 composite

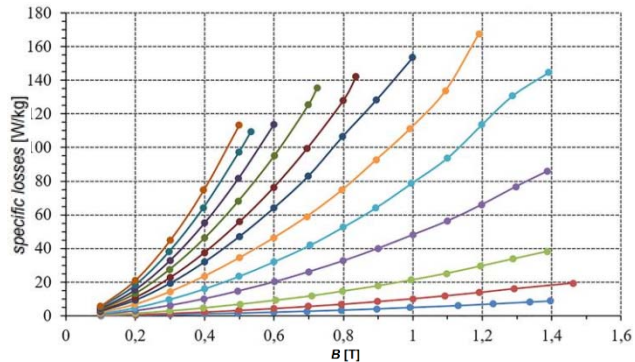
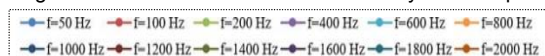


Fig.5. specific losses vs. flux density and frequency characteristics

Numerical analysis of dual star PMSM with soft magnetic composite rotor core

The machine prototype design has been based on stator of series produced eight pole, 2.2 kW asynchronous motor of type SG-132-s8. The original winding of the machine has been replaced by the new fractional slot concentrated winding that excite magnetic field wave of 44 poles in the air gap. The new winding is suited to be supplied by two three phase systems of currents shifted in phase to each other with 30 degrees forming so called real six phase system [2]. In order to determine the machine back electromotive force waveforms (EMF) as well as to study the performance when working as a motor, the dedicated numerical model has been developed in professional FEM package Ansys Maxwell EM. The numerical model of the machine consists of FEM equations describing the magnetic field distribution in 2D space, mechanical equilibrium equation and equations describing the supply system. The properties of applied SMC material (B-H curve shown in Fig. 4 and losses vs. frequency and magnetic flux characteristics from Fig. 5 have been taken into account. The considered domain has been subdivided into about 45 000 triangular elements. The applied FEM mesh has been refined in the air-gap region of the machine. In order to improve model accuracy the geometry of the problem has been reduced out of symmetry of the magnetic circuit. The view of geometry of the machine and applied finite element (FE) mesh have been illustrated in Fig. 6, while major parameters of the machine have been summarized in Table 1.

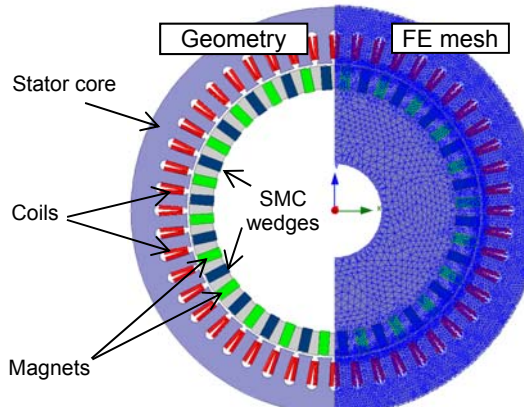


Fig.6. View of the geometry of the machine and applied FE mesh

Table 1. Major parameters of the machine

Outer diameter: 208mm	Number of phases: 6
Number of slots: 48	Stack length: 78mm
Number of poles: 44	Magnets: N42SH

The developed FEM model has been employed to determine the back EMF waveforms as well as to study the machine performance working as a motor. Determined phase and line to line back EMF waveforms at open circuit state and rotor speed equal n_s to 250 rpm have been shown in Figs. 7a) and 8a), respectively. To assess the distortion of determined back EMF waveforms the percentage contents of higher harmonics have been calculated by means of Fast Fourier Transform (FFT) algorithm implemented in own developed software. Obtained results for ABC star have been shown in Figs. 7b) and 8b) for phase and line to line waveforms, respectively. As it can be noted, the phase waveforms contains of third and fifth, seventh and ninth harmonics, while in line to line waveforms the presence of harmonics orders dividable by three is cancelled.

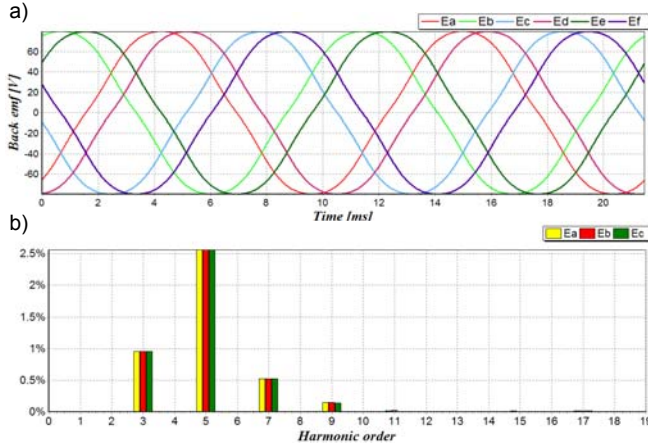


Fig.7. Phase back EMF waveforms a) and its harmonic content for the first star b)

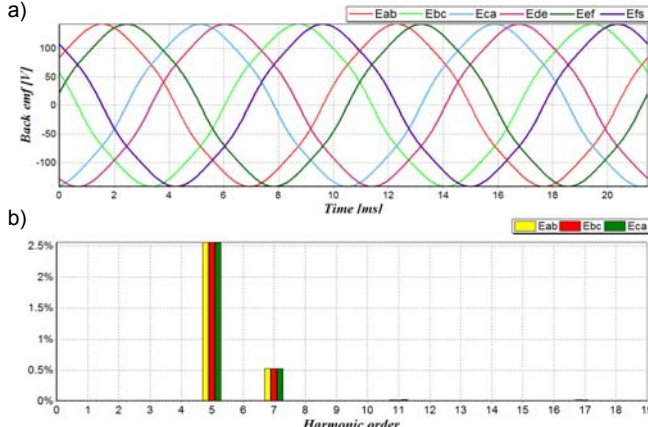


Fig.8. Line to line back EMF waveforms a) and its harmonic content for the first star b)

The performance of the machine working as a motor has been tested for two cases, i.e. normal operation, when both supply voltage stars are active - dual star operation a) and b) operation under drive fault conditions i.e. when one of the supply sources (three phase balanced system) is inactive - disconnected from the motor windings. In both cases the voltage sources supplying the machine were not controlled by means of field oriented control algorithm (so called "open loop operation" mode). Determined phase current waveforms for supply voltage amplitude equal to 7V and frequency 4Hz for single star operation (case b) and dual star operation (case a) have been shown in Fig. 9a)

and 9b), respectively. Calculated electromagnetic torque waveforms for studied cases have been compared in Fig. 10.

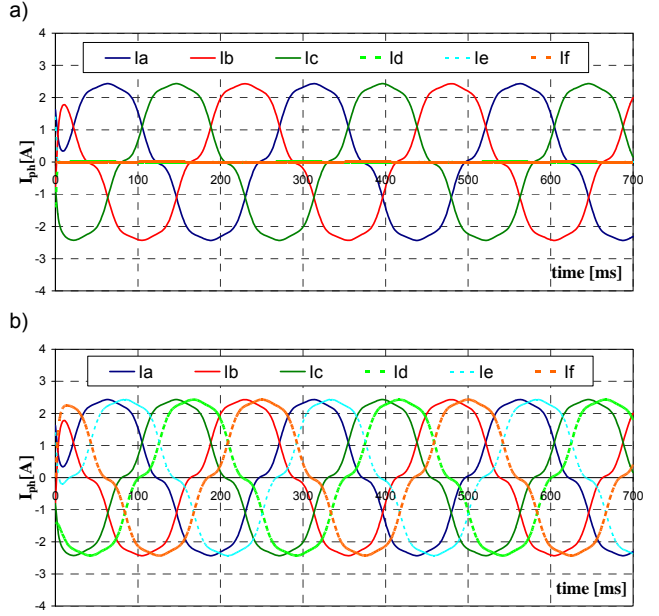


Fig.9. Current waveforms for single star and dual star operation

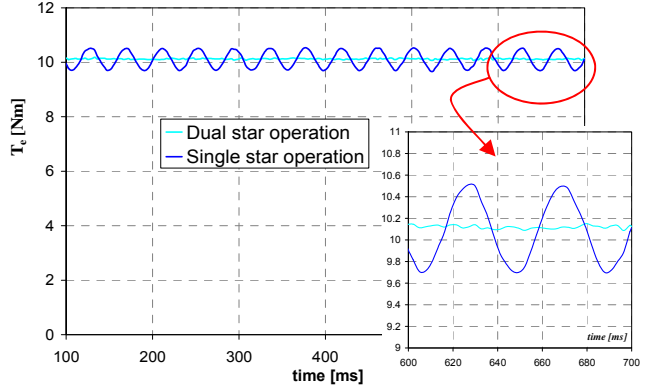


Fig.10. Comparison of electromagnetic torque T_e waveforms for studied cases

As it can be noted, under the drive fault conditions, i.e. for single star operation the torque ripples are significantly higher. However the average value of T_e is equal to applied load torque. Studying the determined current waveforms it can be stated that for applied open loop control mode the phase current waveforms as well as amplitudes for ABC star are not changing significantly when second star (DEF) is being disconnected.

Experimental verification of machine performance under normal and drive fault conditions

The measurements of selected parameters of the developed test machine have performed on special designed research test stand shown in Fig. 11. The stand consists of six phase PMSM machine driven by uniquely designed dual three phase inverter controlled by ALS-1369 DSP based control system, data acquisition system (DAQ) based on National Instrument NI9220 DAQ and DC power system utilizing dual channel TTIQPX600DP programmable DC supply. The diagram and photograph of the developed test stand have been shown in Fig. 11 and 12 respectively.

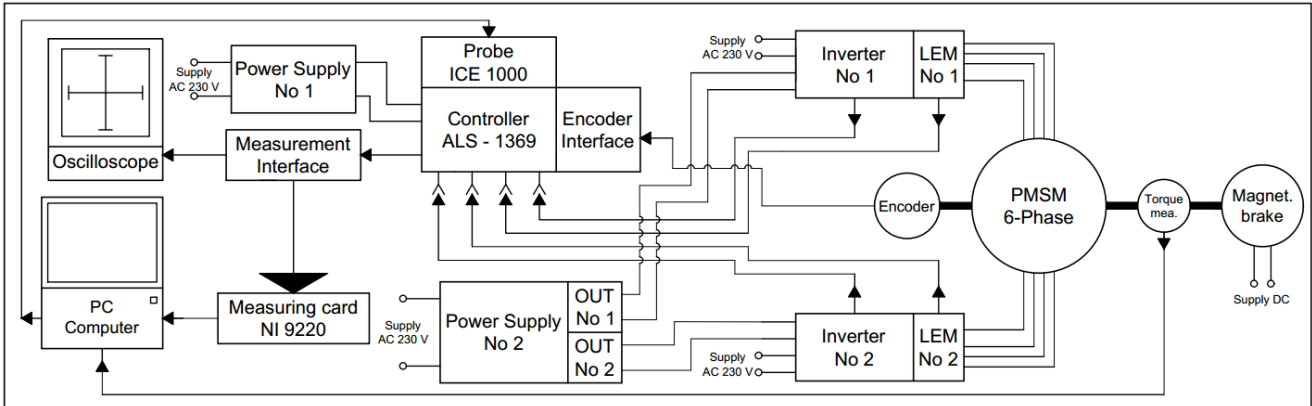


Fig.11. Block diagram of the developed test stand



Fig.12. Developed test stand - photograph (1 - PC for programming and data processing; 2 - supply, DAQ and control system; 3 - six phase PMSM and encoder; 4 – torque measurement device; 5 - magnetorheological brake;)

The dual three phase inverter has been developed using two independent lab-inverters of type P4-500MFE shown in Fig. 13.



Fig.13. Applied P4-50-600 MFE frequency converters

The control system has been based on ALS-1369 DSP development board. To control the dual three phase inverter six independent PWM channels of the ALS-1369 DSP have been used. In the control system two algorithms have been implemented: a) simple open loop six phase voltage source, and b) closed loop field oriented control (FOC). In open loop algorithm the extended to six phase Clarke transformation has been applied, while in FOC six phase PMSM control algorithm both direct and inverse Clarke transformations have been used. The implemented transformations can be described by following transformation matrix equations [7]:

a) extended Clarke transformation:

$$(1) \quad \mathbf{x}_{\alpha\beta} = k \cdot \mathbf{T}_{6f/\alpha\beta} \cdot \mathbf{x}_{6f},$$

$$(2) \quad \mathbf{T}_{6f/\alpha\beta} = \begin{bmatrix} 1 & -\frac{1}{2} & -\frac{1}{2} & \frac{\sqrt{3}}{2} & -\frac{\sqrt{3}}{2} & 0 \\ 0 & \frac{\sqrt{3}}{2} & -\frac{\sqrt{3}}{2} & \frac{1}{2} & \frac{1}{2} & -1 \end{bmatrix},$$

$$(3,4,5) \quad \mathbf{x}_{\alpha\beta} = \begin{bmatrix} x_{\alpha} \\ x_{\beta} \end{bmatrix}, \quad \mathbf{x}_{6f} = \begin{bmatrix} x_A \\ x_B \\ x_C \\ x_D \\ x_E \\ x_F \end{bmatrix}, \quad k = \frac{1}{3},$$

b) extended inverse Clarke transformation:

$$(6) \quad \mathbf{x}_{6f} = \mathbf{T}_{\alpha\beta/6f} \cdot \mathbf{x}_{\alpha\beta},$$

$$(7) \quad \mathbf{T}_{\alpha\beta/6f} = \begin{bmatrix} \cos(0) & \sin(0) \\ \cos\left(\frac{2\pi}{3}\right) & \sin\left(\frac{2\pi}{3}\right) \\ \cos\left(\frac{4\pi}{3}\right) & \sin\left(\frac{4\pi}{3}\right) \\ \cos\left(\frac{\pi}{6}\right) & \sin\left(\frac{\pi}{6}\right) \\ \cos\left(\frac{5\pi}{6}\right) & \sin\left(\frac{5\pi}{6}\right) \\ \cos\left(\frac{9\pi}{6}\right) & \sin\left(\frac{9\pi}{6}\right) \end{bmatrix} = \begin{bmatrix} 1 & 0 \\ -\frac{1}{2} & \frac{\sqrt{3}}{2} \\ -\frac{1}{2} & -\frac{\sqrt{3}}{2} \\ \frac{\sqrt{3}}{2} & \frac{1}{2} \\ -\frac{\sqrt{3}}{2} & \frac{1}{2} \\ 0 & -1 \end{bmatrix},$$

where: $\mathbf{x}_{6f}, \mathbf{x}_{\alpha\beta}$ – are the state vectors in natural and orthogonal reference frame, respectively, \mathbf{T} – transformation matrix, k – power scaling coefficient.

In the closed loop algorithm rotor position has been measured by use of KublerK8-F3653-4518-C71. The applied encoder and the tested machine are shown in the Fig. 12.

Verification has been carried in two operation modes under open loop control scheme. In the first variant, only one star of the tested machine was supplied (single star operation SSO), while in the second variant, both stars were supplied (DSO). In both cases machine has been loaded by magnetorheological brake of constant value of torque equal to 10 Nm. All of tests have been conducted in “open loop mode”, i.e. no control loop for the i_d , i_q currents has been applied. The supply frequency has been set to 4 Hz and amplitude of the phase voltages was equal to about 6V.

Measured torque waveforms for SSO and DSO conditions have been compared in Fig. 17, while acquired voltage and current waveforms for single star operation

have been shown in Fig. 14a) and 14b), respectively. The phase voltage and phase current waveforms for dual star operation have been shown in Fig. 15 and 16.

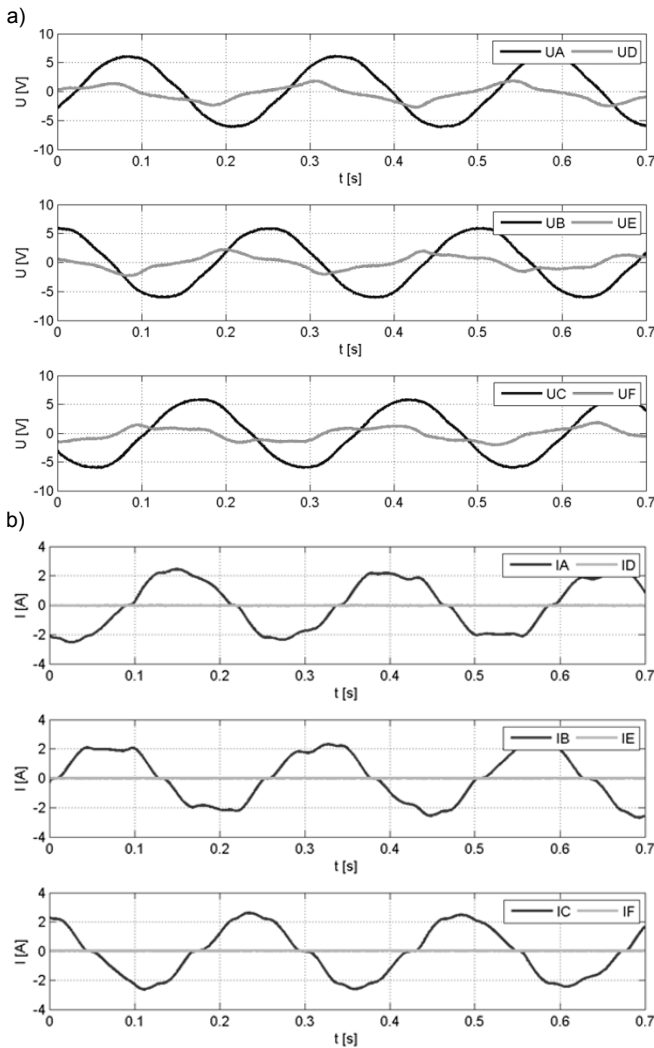


Fig.14. Voltage (a) and current (b) waveforms for single star operation

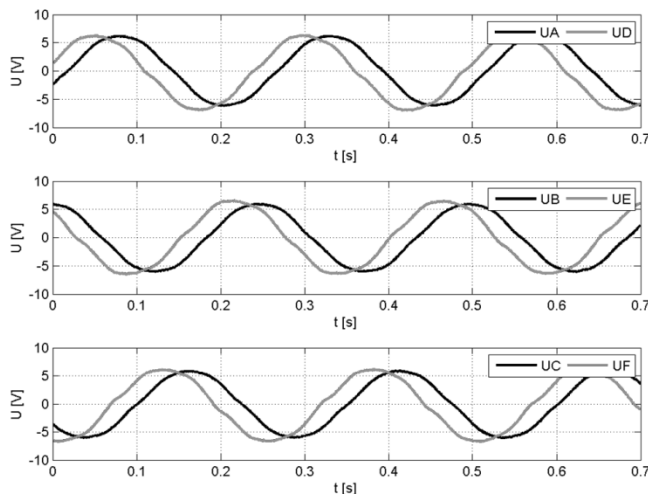


Fig.15. Voltage waveforms for dual star operation

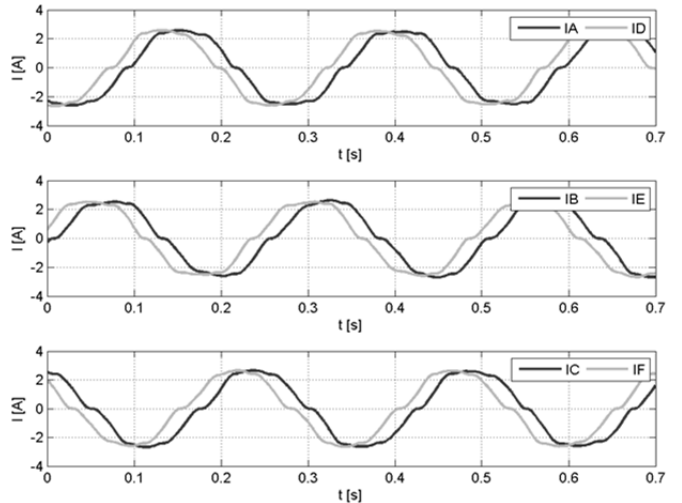


Fig.16. Current waveforms for dual star operation

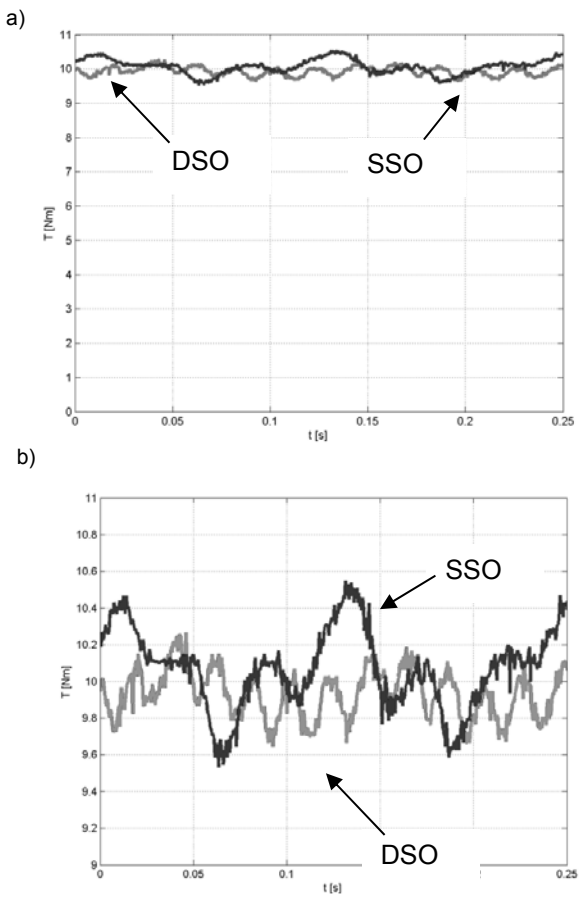


Fig.17. Acquired torque waveforms for: single star operation (SSO) and dual star operation (DSO)

It should be noted, that as expected under three phase supply mode the motor exhibit higher torque pulsation than under six phase operation. However, the level and frequency of the torque ripples differs from simulated values. The main reasons in our opinion are lack of high inertia wheel in the measuring system and open loop control mode.

Conclusion

The paper presents research focused on analysis of the multiphase PMSM with fractional slot concentrated winding and rotor back iron made of soft magnetic composite

Somaloy 500. The manufacturing process and magnetic properties of Somaloy 500 have been briefly discussed. The numerical model of the studied machine has been developed and used in analysis of motor performance. The normal operation of the machine (i.e. supplied by dual star six phase system) as well as supply fault condition (i.e. machine supplied by single star three phase system) have been examined. Presented results show that under supply fault condition machine exhibit higher electromagnetic torque ripple level comparing to normal operation of the machine. To verify these findings as well as to prove model accuracy the machine prototype has been designed, built and tested on developed experimental setup. To test the machine prototype the customized six phase supply system has been developed. Commissioned supply system is based on application of two three phase inverters controlled by common DSP control board. Due to the increased number of phases of the tested machine direct application of the standard control algorithms was not possible. The customized algorithms have been developed and employed in the control system. Most crucial was the correct representation of the current space vector. For this need the direct and reverse transformations adapted for the six-phase systems and based on the Clarke approach were determined and implemented into the control system.

Researches related to the analysis and synthesis of multiphase permanent magnet synchronous machines with fractional slot concentrated windings are still ongoing. The current objective is to create a complex drive application adapted to the power supply and control of machines with an increased number of phases allowing for testing the machine performance in closed loop vector control algorithm. The results of these works will be the scope of further publications of the authors.

Authors: dr hab. inż. Cezary Jędryczka, Poznan University of Technology, Institute of Electrical Engineering and Electronics, Piotrowo 3a St., 60-965, Poznan, Poland,

E-mail: cezary.jedryczka@put.poznan.pl.

mgr inż. Dariusz Kapelski, Tele and Radio Research Institute, Ratuszowa 11 St., 03-540 Warsaw, Poland,

E-mail: dariusz.kapelski@itr.org.pl, dr inż.

dr inż. Dariusz Janiszewski, Poznan University of Technology, Institute of Electrical Engineering and Electronics, Piotrowo 3a St., 60-965, Poznan, Poland,

E-mail: dariusz.janiszewski@put.poznan.pl.

dr inż. Michał Krystkowiak, Poznan University of Technology, Institute of Electrical Engineering and Electronics, Piotrowo 3a St., 60-965, Poznan, Poland,
E-mail: michal.krystkowiak@put.poznan.pl.
mgr inż. Dawid Danielczyk, Poznan University of Technology, Institute of Electrical Engineering and Electronics, Piotrowo 3a St., 60-965, Poznan, Poland,
E-mail: dawid.p.danielczyk@doctorate.put.poznan.pl

REFERENCES

- [1] A.M. EL-Refaie, (2010), "Fractional-Slot Concentrated-Windings Synchronous Permanent Magnet Machines: Opportunities and Challenges", IEEE Transactions on Industrial Electronics, vol. 57, no. 1, 2010, pp. 107-121, doi: 10.1109/TIE.2009.2030211.
- [2] C. Jedryczka, (2017), "Comparative analysis of the three- and six-phase fractional slot concentrated winding permanent magnet machines", COMPEL - The International Journal For Computation and Mathematics in Electrical and Electronic Engineering, vol. 36, no. 3, pp. 811-823.
- [3] F. Magnussen, H. Lendenmann, (2007), "Parasitic Effects in PM Machines With Concentrated Windings", IEEE Transactions on Industry Applications, vol. 43, no. 5, pp. 1223-1232, 2007, doi: 10.1109/TIA.2007.904400.
- [4] D. Biało, (2001), „Wytwarzanie kompozytów w procesach metalurgii proszków (Manufacturing of composites by the powder metallurgy route)”, Composites 1, pp. 89–92 (2001).
- [5] M. Najgebauer , J. Szczęgłyowski, B. Ślusarek, M. Przybylski, A. Kaplon, J. Rolek (2018), "Magnetic Composites in Electric Motors", In: Mazur D., Gołębowski M., Korkosz M. (eds) Analysis and Simulation of Electrical and Computer Systems. Lecture Notes in Electrical Engineering, vol 452. Springer, Cham.
- [6] C. Xiao, W. Jiabin, P. Vipulkumar, L. Panagiotis, (2016) "A Nine-Phase 18-Slot 14-Pole Interior Permanent Magnet Machine With Low Space Harmonics for Electric Vehicle Applications", IEEE Transactions on Energy Conversion, vol. 31, no. 3, September 2016.
- [7] M. Janaszek, (2016), "Structures of vector control of n-phase motor drives based on generalized Clarke transformation", Bulletin of the Polish Academy of Sciences Technical Sciences, vol. 64, no. 4, 2016, doi: 10.1515/bpasts-2016-0094.
- [8] P. Di Barba, M. Mognaschi, S. Wiak, M. Przybylski, B. Ślusarek, (2018), "Optimization and measurements of switched reluctance motors exploiting soft magnetic composite", International Journal of Applied Electromagnetics and Mechanics, vol. 57, no. S1, pp. 83-93, 2018.